

A POSITIONING LOCKHOLES OF CONTAINER CORNER CASTINGS METHOD BASED ON IMAGE RECOGNITION

Yang Shen^{1,2*}

Weijian Mi³

Zhiwei Zhang⁴

¹Institute of Logistics Science & Engineering, Shanghai Maritime University, Shanghai 201306, China

²Higher Technical College, Shanghai Maritime University, China

³Container Supply Chain Tech. Engineering Research Center, Shanghai Maritime University, China

⁴Shanghai Weiguo Port Equipment Company Limited

* corresponding author

ABSTRACT

This article proposes a method of locating and recognizing lockholes in shipping container corner castings. This method converts the original image of the containers captured by a camera into the HSV (Hue, Saturation, Value) color space. To reduce the influence of the surface color of the containers and lights from the environment on the locating and recognizing algorithm, most noisy points of the image are filtered by binarization and a morphology opening operation to make the features of the containers clearer in the image. Thus, the container body can be separated from the total image. Then, the position and size of the corner castings are defined through calculation based on the international standard of the shipping container size. Lastly, by using this method, we can locate the corner casting in the image by using the General Hough Transform fitting algorithm onto ellipses.

Keywords: Lockholes of container corner; HSV; Lockholes positioning; Hough transformation

INTRODUCTION

In recent years, with rapid developments in export and import trading and the shipping market, major container terminals in the world are facing the challenge of rapid growth in container throughput capacity. To cope with the rising freight volume, the need for larger container vessels and operation machines is becoming more evident [1-2]. However, the need to maximize container ship stowage capacity and minimize the time for handling a ship in port result in significant pressure on increasing cargo handling efficiency. Thus, automation container terminals have become key projects all over the world.

Following this trend, large-scale machinery in automation ports is more automated and intelligent [3-5]. Earlier, the self-direction function of automated terminal crane equipment was usually possessed by the encoder, which may not be

as flexible or efficient as the directing method of machine vision. Nowadays, more researchers are using various ways to automate terminal crane equipment in their projects. The machine vision system has been one of the most popular ways to actualize automation in recent years [6-8].

The terminal machine vision system was originally applied to recognize case numbers on shipping containers [9]. Later automated recognition systems tracked and located large targets such as containers and container trucks. However, it is still difficult to recognize or posit on tiny but important features of container targets. For example, an automated recognition system cannot identify small accessories of containers such as the precise lockhole position on a container corner casting. It is also difficult to judge if the lock is attached to the container.

Hence, this article researches the identification of lockholes of containers based on a machine vision system. The purpose

of this paper is to quickly locate containers and specifically positing the lockholes of containers picture by the algorithm. After determining the specific positions of the lockholes, the container checking system will be able to calculate the positions of other key accessories and check their situations automatically.

Mi Chao et al. presented a rapid automated vision system for container corner casting recognition by using histograms of oriented gradients (HOG) descriptors [10]. Chen Mo et al. proposed a method to extract the container code characters (CCCs) when all 11 CCCs appear in an image and when some CCCs are missing. This method can estimate the positions of missing characters [11].

Kumano, S et al. used a character recognition scheme based on a dynamic design method to recognize different character string layouts in container marks or numbers [12]. This scheme can filter various container colors. Abbate Stefano presented a nonconventional approach in which each container was equipped with nodes that used wireless communication to detect neighbor containers, and to send proximity information to a base station [13]. The positions of containers can be determined by the base station.

Wu and Wei et al. proposed a segmentation-based approach to recognize characters in single-character blocks, and a hidden Markov model (HMM)-based method for multi-character blocks [14].

IMAGE PREPROCESSING

At container terminals, camera locations may influence the angles in which photos are taken. This may cause slopes, zooms, and deformations of the targets, as shown in Figure 1. This kind of deformation will later influence processing images directly.

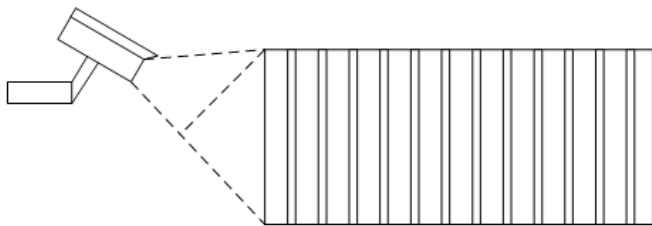


Fig. 1. Camera installation position for image recognition

In order to correct these deformations, the original image of a container will be sized by geometric transformation. During our image processing, the original image will be adjusted by linear and nonlinear transformations including affine transformations of zoom, rotation, and translation, and perspective transformations that may correct twist distortions [15] [16]. As formula 1 indicates, the perspective transformation will be conducted using a 3×3 matrix. The result of the perspective transformation will also depend on this matrix.

$$[wx, wy, w] = [u, v, 1] \begin{bmatrix} a_{11} & a_{12} & a_{13} \\ a_{21} & a_{22} & a_{23} \\ a_{31} & a_{32} & a_{33} \end{bmatrix} \quad (1)$$

In the expression, u, v are the coordinates of the container's original image, and x, y are the coordinates after transformation.

The transformation matrix $\begin{bmatrix} a_{11} & a_{12} & a_{13} \\ a_{21} & a_{22} & a_{23} \\ a_{31} & a_{32} & a_{33} \end{bmatrix}$ contains three sections: linear transformation section $\begin{bmatrix} a_{11} & a_{12} \\ a_{21} & a_{22} \end{bmatrix}$ translation transformation section $[a_{31} \ a_{32}]$, and perspective transformation section $[a_{13} \ a_{23}]^T$.

In order to eliminate image distortion, the distortion parameter of the perspective transformation will be demarcated manually before recognizing the lockholes of the corner casting. Thus, we gain the best visual result of the original container image taken by cameras through the above transformations.

Figure 2 compares the images of a container before and after the perspective transformation.



Fig. 2. Comparison between source image and perspective transformed image

In the practical loading and unloading operation process at ports, the brightness of the container body in the original image is almost the same as the background, but the container colors may differ because of various shipping companies and the different type of cargo inside. Hence, to eliminate the influence of different container surface colors on the recognition algorithm, we convert the image from the original RGB color space into the HSV color space [17]. Our computers locate the container body in the HSV color space faster by using our algorithm, and then find the corner castings in the image.

The following formula 2 processes the original image from the RGB color space into the HSV color space.

$$H = \begin{cases} \frac{G-B}{Max-Min} * 60^\circ, (R = Max) \\ \left(2 + \frac{B-R}{Max-Min}\right) * 60^\circ, (G = Max) \\ \left(4 + \frac{R-G}{Max-Min}\right) * 60^\circ, (B = Max) \end{cases} \quad (2)$$

$$S = \frac{Max - Min}{Max}$$

$$V = Max$$

In the expression, the R, G, and B components are normalized into the range of [0,1]. In addition, *Max* is the highest number among these three components, and is the smallest number. In the result, H is the hue angle degree, which is between 0°–360°. S and V represent the saturation level and brightness, respectively, which are between 0–1. Figure 3 shows the container image after being converted into the HSV color space.

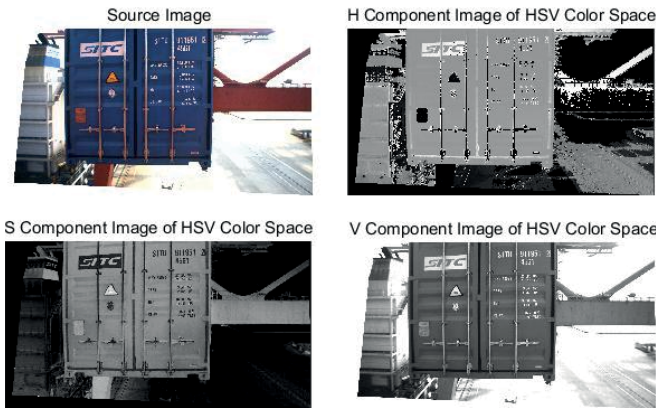


Fig. 3. HSV color space of container image

After changing into the HSV color space, we use the S channel image to process other transformations because the H channel may be affected by the container’s surface color. In addition, the V channel may be affected by environmental lighting. In order to separate the container body from the background in the image, the S channel image is by binarization. Each pixel has only one S value in the S channel, which equals a grayscale image. Here, grayscale is a color value between 0–255. In this experiment, we use formula 3 for the binary S channel image, in which $f(x, y)$ represents the grayscale value, and s is the threshold value of binarization. Here, we take s as 120.

$$f(x, y) = \begin{cases} 0, & f(x, y) < s \\ 255, & f(x, y) > s \end{cases} \quad (3)$$

After binarization, many interfering points from the background environment still remain in the image, but these points can be filtered through a morphology opening operation.



Fig. 4. Binarization and opening operation of S component image

In Figure 4, the features of the container are clearer after being denoised by binarization in the S channel and the morphology opening operation [18].

LOCATING CONTAINERS IN IMAGE

After binarization and filtering, the algorithm is able to precisely locate the container body in the binarization image using projective histograms.

The calculation steps are as follows:

1. We projected the binarization image in the vertical and horizontal directions [19]. The projected curve is shown in Figure 5.

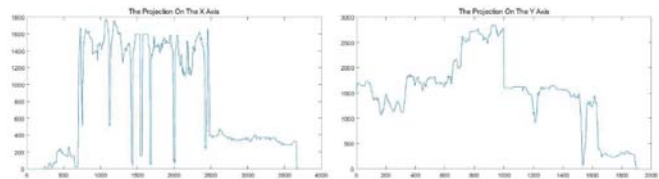


Fig. 5. Projection on X and Y axes

2. As formula 4 indicates, first we choose the proper threshold based on the value of the peak area. Then, we use a binary threshold on these two projection curves. In other words, we choose a specific threshold value. Then, any point that is bigger than this threshold value will be represented as 1, and any other smaller value will be represented as 0. The result of the threshold operation is shown in Figure 6.

$$f(x) = \begin{cases} 1, & \text{if } f(x) > t \\ 0, & \text{otherwise} \end{cases} \quad (4)$$

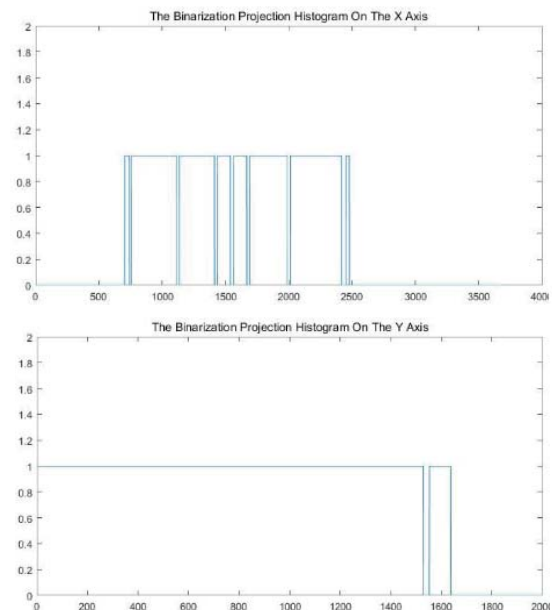


Fig. 6. Binarization projection histogram

3. We obtain the four limitation coordinates Xmin, Xmax, Ymin and Ymax of the container by calculating the location coordinates of the first rise edge and the last fall edge.

4. As shown in Figure 7, according to the square shape confirmed by the four limitation coordinates, the container shape can be cut out in the S channel image.



Fig. 7. Cut out container target

LOCKHOLE RECOGNITION

In order to eliminate the influence of various marks on the container surface on the recognition algorithm, and to improve the calculating speed, the corner casting shape is separated from the total image. ISO 6346 regulates the size of corner castings. The height of a corner casting is assumed to be h , and the width-height ratio of a standard corner casting is λ . Thus, the width of the corner castings is λh . The alignment and segmentation of two downside corner castings is expressed in formula 5 to adjust the error.

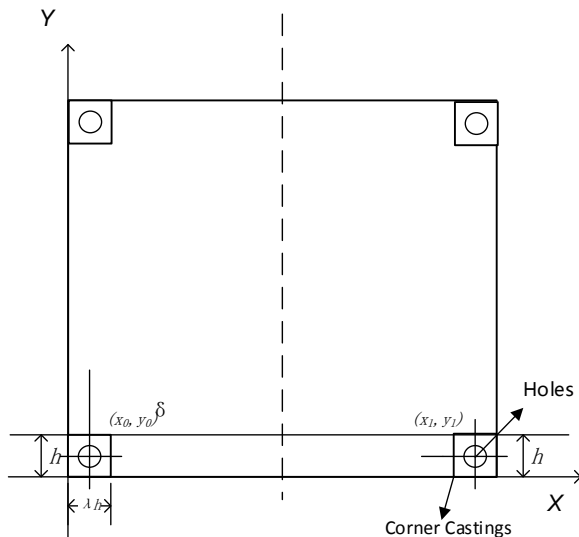


Fig. 8. Size of container corner castings.

$$\begin{cases} x_0 = \lambda(h + \delta) \\ y_0 = h + \delta \\ x_1 = W - \lambda(h + \delta) \\ y_1 = H - (h + \delta) \end{cases} \quad (5)$$

In the above expression, are the coordinates of the lower left and right corner castings. λ is the width-height ratio,

as mentioned earlier in this paper. In ISO 6346, the corner casting size is defined as 178 (l) \times 162 (w) \times 118 (h). Thus, $\lambda=1.37$. W and H are, respectively, the width and height of the container's segmented image, and δ is the error parameter that can be set according to the practical situation.

Based on the sizes that we determined above, the corner casting figure can be separated from the container image. The isolated corner casting image will be grayscaled and then binarized, and will also be processed by a Canny edge detector. Last, the edge features of the corner casting will be extracted [20]. Afterward, the outline pixels will be analyzed so that connected pixel points will be determined as one outline. In doing so, the corner casting shape will be presented as outline curves.

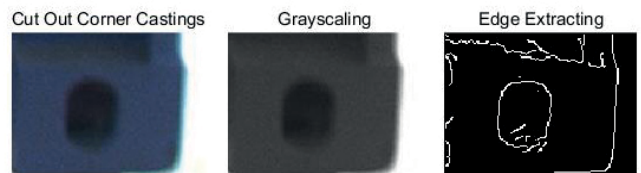


Fig. 9. Corner casting image processing

A Hough transformation can be applied in detecting circles based on the principles of the algorithm. This is called the General Hough Transform. There is one additional parameter radius R in the circle standard expression. To recognize a round shape by the algorithm, the parameter plane will be developed into a three-dimensional space $x - y - R$. Every pixel point in the picture corresponds to a circle in a parameter space with a different radius value. In the end, the entire figure in the parameter space will be presented as a circular cone. Furthermore, the General Hough Transform can be applied to ellipses as well as variants of circles. The following are parameter expressions of ellipse shapes:

$$\begin{cases} x = \alpha \cos T \cos \theta - \beta \sin T \sin \theta + p \\ y = \alpha \cos T \sin \theta + \beta \sin T \cos \theta + q \end{cases} \quad (6)$$

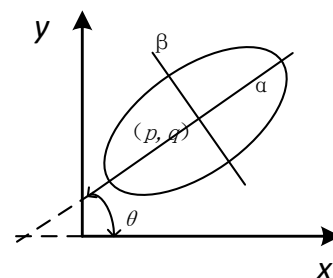


Fig. 10. Ellipse free parameter representation.

As shown in Figure 10, each ellipse has a total of five free parameters, including the center coordinates, major and minor axis radius, and the fleet angle degree. Under usual circumstances, to solve these five free parameters, we need at least five boundary coordinates. During the recognition process for container lockholes, the algorithm will detect

elliptical shapes on a closed outline in order. Hence, the center point, major and minor axis radius, and fleet angle of the lockhole shape will be determined by the program. The ellipses of lockholes will be redrawn according to the parameter set. The final detecting result is shown in Figure 11.

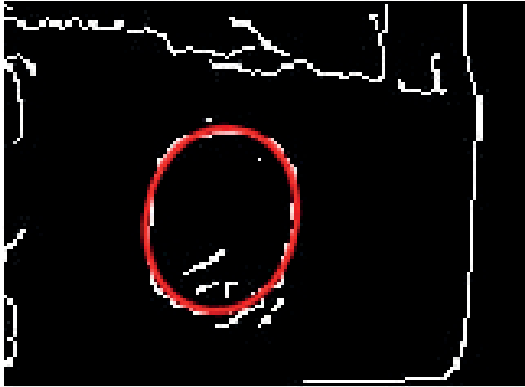


Fig. 11. Hole of container corner recognition results

EXPERIMENTAL RESULTS AND ANALYSIS

The experiment of this article was completed in Taicang Port, Jiangsu Province, China. Four sets of samples were collected and divided by two sizes of containers and different lighting situations: 20-foot container in daylight, 40-foot container in daylight, 20-foot container at night, and 40-foot container at night. Our researchers picked 250 samples from each set to test the adaptability of our algorithm in an entire-day situation. The results are listed in the following Table.

Tab. 1. Experimental results.

Lightness	Container Size	Samples Quantity	Effective samples quantity	Correct Amount	Recognition rate	Detecting time (ms)
Daytime	20	250	486	466	95.9%	300
	40	250	473	458	96.8%	
Nighttime	20	250	461	432	93.7%	
	40	250	465	433	93.1%	

In practical application, the two upper lockholes are usually covered by the hangers from port machines. Thus, only the two lower lockholes will be recognized by the algorithm. Because the timing of taking pictures is hard to control, the effective sample quantity cannot reach the ideal sample quantity. Table 1 reveals the actual number of lockholes that we obtained.

An analysis of this result indicates that the algorithm effectively recognizes lockholes in daylight. The recognition rate can be over 95%, especially in sufficient light conditions. Meantime, the recognition rate for nighttime arrives 93% which is lower than daytime rate because the light sources in the port at nighttime are fill lights pointed in various directions. These complicated lighting conditions cause different degrees of shadow on the lockholes and around the area. This impacts the locating and recognizing function.

In this experiment, we set different parameter thresholds in the detecting stage for different sizes of containers. According to the results Table, the difference between the 20-foot and 40-foot containers is smaller in the daytime. At night, the lockholes on 20-foot containers are smaller and are more susceptible to lightness. Thus, the recognition rate for a 20-foot container at night is below the rate of the 40-foot container.

With regard to the effectivity of this algorithm, the average recognition time is approximately 300 ms, which satisfies the needs of real-time performance in automatic ports.

CONCLUSION

Machinery vision technology is important when actualizing automatic container ports, and is gaining attention from other researchers. This article studies the recognition of container lockholes using practical experience. It also introduces the current research direction and situation in automatic container ports. We explain the basic process of lockhole recognition in detail, including image preprocessing, isolating the container body image, and locating lockholes. Then, we show the specific operation steps. Using an entire-day practical test and various parameter calibrations, this system qualifies for practical application and performs well, as proven by experimental results.

ACKNOWLEDGEMENT

This research was supported by the National Natural Science Foundation of China (No.61540045), the Science and Technology Commission of Shanghai Municipality (No.15YF1404900, No.14170501500), Ministry of Education of the PR China (No.20133121110005), Shanghai Municipal Education Commission (No. 14ZZ140), Shanghai Maritime University (No.2014ycx040).

REFERENCES

1. Lam Jasmine Siu Lee, Song Dong-Wook, "Seaport network performance measurement in the context of global freight supply chains", Polish Maritime Research, Vol. 20, SI. 1, pp. 47-54 (2013)
2. Gamal Abd El-Nasser A. Said, El-Sayed M. El-Horbaty, "An intelligent optimization approach for storage space allocation at seaports: A case study", 2015 IEEE Seventh International Conference on Intelligent Computing and Information Systems (ICICIS), pp. 66-72 (2015)
3. Song Su, "Ship emissions inventory, social cost and eco-efficiency in Shanghai Yangshan port", ATMOSPHERIC ENVIRONMENT, Vol. 82, pp. 288-297 (2014)
4. Mi Chao, Huang Youfang, Liu Haiwei, Shen Yang, Mi Weijian. "Study on Target Detection & Recognition Using

- Laser 3D Vision System for Automatic Ship Loader,” *Sensor & Transducers*, Vol. 158, No.11, pp. 436-442 (2013)
5. Yun Xie, Qifan Bao, Zhenqiang Yao, Zhongxiong Ge, Zhengchun Du, “First automatic empty container yard with no operator in China”, *Technology and Innovation Conference, 2006. ITIC 2006. International*, pp. 1509-1513 (2006)
 6. Mi Chao, Shen Yang, Mi Weijian, Huang Youfang, “Ship Identification Algorithm Based on 3D Point Cloud for Automated Ship Loaders”, *Journal of Coastal Research*, SI.73, pp.28-34 (2015)
 7. Mi Chao, Zhang Zhiwei, He Xin, Huang Youfang, Mi Weijian, “Two-stage classification approach for human detection in camera video in bulk ports”, *POLISH MARITIME RESEARCH*, Vol. 22, pp. 163-170 (2015)
 8. Mi Chao, He Xin, Liu Haiwei, Huang Youfang, Mi Weijian, “Research on a Fast Human-Detection Algorithm for Unmanned Surveillance Area in Bulk Ports”, *MATHEMATICAL PROBLEMS IN ENGINEERING* (2015)
 9. M. Goccia, M. Bruzzo, C. Scagliola, S. Dellepiane, “Recognition of container code characters through gray-level feature extraction and gradient-based classifier optimization”, *Document Analysis and Recognition*, pp. 973-977 (2003)
 10. Mi Chao, Zhang Zhiwei, Huang Youfang, Shen Yang, “A Fast Automated Vision System for Container Corner Casting Recognition”, *Journal of Marine Science and Technology - Taiwan*, Vol.24, No.1, pp.54-60 (2016)
 11. Chen Mo, Wu Wei, Yang Xiaomin, He Xiaohai, “Hidden-Markov-Model-Based Segmentation Confidence Applied to Container Code Character Extraction”, *IEEE TRANSACTIONS ON INTELLIGENT TRANSPORTATION SYSTEMS*, Vol. 12, No. 4, pp. 1147-1156 (2011)
 12. Kumano S., Miyamoto K., Tamagawa M., et al., “Development of a container identification mark recognition system”, *ELECTRONICS AND COMMUNICATIONS IN JAPAN PART II-ELECTRONICS*, Vol. 87, No. 12, pp. 38-50 (2004)
 13. Abbate, Stefano, Avvenuti, Marco, Corsini, Paolo, et al., “An Integer Linear Programming Approach for Radio-Based Localization of Shipping Containers in the Presence of Incomplete Proximity Information”, *IEEE TRANSACTIONS ON INTELLIGENT TRANSPORTATION SYSTEMS*, Vol. 13, No. 3, pp. 1404-1419 (2012)
 14. Wu Wei, Liu Zheng, Chen Mo, “A New Framework for Container Code Recognition by Using Segmentation-Based and HMM-Based Approaches”, *INTERNATIONAL JOURNAL OF PATTERN RECOGNITION AND ARTIFICIAL INTELLIGENCE*, Vol. 29, No. 1, 2015
 15. Yamashita Yukihiro, Wakahara Toru, “Affine-transformation and 2D-projection invariant k-NN classification of handwritten characters via a new matching measure”, *PATTERN RECOGNITION*, Vol. 52, pp. 459-470 (2016)
 16. Alzati Alberto, Carlos Sierra Jose, “Special birational transformations of projective spaces”, *ADVANCES IN MATHEMATICS*, Vol. 289, pp. 567-602 (2016)
 17. Silva A. S., Severgnini F. M. Q., Oliveira M. L., et al., “Object Tracking by Color and Active Contour Models Segmentation”, *IEEE LATIN AMERICA TRANSACTIONS*, Vol. 14, No. 3, pp. 1488-1493 (2016)
 18. Pezeshk Aria, Tutwiler Richard L., “Automatic Feature Extraction and Text Recognition From Scanned Topographic Maps”, *IEEE TRANSACTIONS ON GEOSCIENCE AND REMOTE SENSING*, Vol. 49, No. 12, pp. 5047-5063 (2011)
 19. Kim H., Johnson JT., “Radar images of rough surface scattering: Comparison of numerical and analytical models”, *IEEE TRANSACTIONS ON ANTENNAS AND PROPAGATION*, Vol. 50, No. 2, pp. 94-100 (2002)
 20. Yasmin Jaseema, Sathik Mohamed, “An Improved Iterative Segmentation Algorithm using Canny Edge Detector for Skin Lesion Border Detection”, *INTERNATIONAL ARAB JOURNAL OF INFORMATION TECHNOLOGY*, Vol. 12, No. 4, pp. 325-332 (2015)
 21. Lu Tingting, Hu Weiduo, Liu Chang, “Effective ellipse detector with polygonal curve and likelihood ratio test”, *IET COMPUTER VISION*, Vol. 9, No. 6, pp. 914-925 (2016)
 22. Fornaciari Michele, Prati Andrea, Cucchiara Rita, “A fast and effective ellipse detector for embedded vision applications”, *PATTERN RECOGNITION*, Vol. 47, No. 11, pp. 3693-3708 (2014)

CONTACT WITH THE AUTHORS

Yang Shen

Institute of Logistics Science & Engineering
Shanghai Maritime University
Shanghai 201306
CHINA

Higher Technical College
Shanghai Maritime University
Shanghai 201306
CHINA